

Morphological and Ultrastructural Comparative Analysis of Bone Tissue After Er:YAG Laser and Surgical Drill Osteotomy

Dragana Gabric Panduric, DDS, PhD,¹ Ivona Bago Juric, DDS, PhD,² Svetozar Music, PhD,³ Krešimir Molčanov, PhD,⁴ Mato Sušic, DDS, PhD,¹ and Ivica Anic, DDS, PhD²

Abstract

Objective: The purpose of this study was to analyze morphological, chemical, and crystallographic changes of bone tissue after osteotomy performed with an erbium:yttrium-aluminium-garnet (Er:YAG) laser and a low speed pilot drill. **Materials and methods:** Bone blocks were prepared from porcine ribs, and on each block, two tunnel preparations were performed using the Er:YAG laser (pulse energy: 1000 mJ, pulse duration: 300 μ s, pulse repetition rate: 20 Hz) or the low-speed surgical pilot drill. The morphological changes of the cortical and the spongy surface of the tunnel preparations were analyzed under the field emission scanning electron microscopy (FE-SEM) at low and high resolution. The distribution and the level of chemical elements in the treated surfaces were evaluated by qualitative and semiquantitative energy dispersive x-ray analysis (SEM-EDX). Diffraction x-ray analysis was used to detect any differences and thermally induced modifications of hydroxyapatite crystals. **Results:** FE-SEM revealed sharp edges of the Er:YAG preparations, with empty intertrabecular spaces and no signs of carbonization. In the drill group, the surface of the preparations was smooth, completely covered with smear layer and microcracks, and with hairy-like irregularities on the edges. SEM-EDX analysis did not reveal any differences in the number of specific chemical elements between the laser and the drill group. There were no thermally induced modifications of hydroxyapatite crystal structure in the bone tissue in either group. **Conclusions:** The Er:YAG laser ablation did not cause any chemical or crystallographic changes of the bone tissue. Compared with the drill, Er:YAG laser created well-defined edges of the preparations, and cortical bone had no smear layer.

Introduction

OSTEOTOMY PROCEDURES in oral and maxillofacial surgery are usually performed with drills, mills, oscillating saws, and chisels.^{1,2} However, the use of these instruments can cause deposition of metal shavings and increase of the focal temperature of regions undergoing the procedure.^{2,3} Although the mechanically rotating instruments are fitted with an internal cooling system during the procedure, it is not possible to prevent thermal damage of the surrounding bone tissue completely.⁴ Furthermore, by using the instruments, there is a higher risk for damaging the surrounding and enveloped tissues in more complicated anatomical locations.²

Over the last several decades, the use of different types of high-energy lasers in bone surgery has been explored.^{2,5,6}

The erbium:yttrium-aluminium-garnet (Er:YAG) laser, which emits radiation of wavelength 2.94 μ m, is strongly absorbed in water and hydroxyapatite, causing photothermal reaction and photoablation.^{6,7} Because of many advantages such as narrow and precise cut geometry, reduced risk of adjacent tissue injury, high bactericidal and detoxification effect, absence of massive bone four and metal abrasion, reduced tissue bleeding, and absence of vibration during procedures,^{6,8} the Er:YAG laser has been reported as suitable for clinical bone surgery.⁷ Moreover, by using short-pulse Er:YAG laser systems with water irrigation, it is possible to cut bone more rapidly,^{8,9} and without significant thermal damage of the surrounding tissue (charring or necrosis). Consequently, wound healing is comparable to or even faster than osteotomies performed with drills or oscillating saws.^{7,9–16} Histological and

¹Department of Oral Surgery, School of Dental Medicine, University of Zagreb, Zagreb, Croatia.

²Department of Endodontics and Restorative Dentistry, School of Dental Medicine, University of Zagreb, Zagreb, Croatia.

³Division of Materials Chemistry, Laboratory for Synthesis of New Materials, Ruđer Bošković Institute, Zagreb, Croatia.

⁴Division of Physical Chemistry, Laboratory for Chemical and Biological Cristallography, Ruđer Bošković Institute, Zagreb, Croatia.

electronic microscopic evaluation of the Er:YAG bone preparations has shown minimal thermal damage to bone tissue, precise cutting, and rapid osseous healing.^{7,9}

However, the application of the Er:YAG laser has not been accepted in everyday clinical practice yet. One of the reasons is the lack of studies on the characteristics of the bone tissue irradiated at different physical laser parameters.⁸ The aim of the present study was to analyze the morphological, chemical, and crystallographic characteristics of bone tissue after Er:YAG laser ablation and low-speed pilot drill osteotomy using field emission scanning electron microscopy (FE-SEM), energy dispersive x-ray analysis (SEM-EDX), and x-ray diffraction analysis (XRD).

Materials and Methods

Specimens

The experimental study was performed on 30 freshly harvested sternal parts of porcine ribs, which were split into two halves with sagittal osteotomy. Each half of the rib was split into equal segments ($2.0 \times 1.0 \times 0.5$ cm), with approximately same thickness of cortical and spongy parts, using a water-cooled slow-speed diamond disk (Isomet 1000; Buehler International, Inc., Lake Bluff, IL), set at 250 rpm with a 100 g load. Finally, the bone blocks were stored in 0.1% thymol solution until use, in order to prevent dehydration of the samples and to reduce bacterial growth. The thickness of the blocks was 4.6 ± 0.7 mm, including cortical (1.3 ± 0.4 mm) and spongy parts (3.3 ± 0.6 mm). Before the experimental procedures, the samples were dried with compressed air and adjusted to room temperature.

Experimental procedures

The research protocol was approved by the Local Ethics Committee (47/2008). Each bone block was divided into two equal parts with a line parallel to the shorter side of the block. At each part of the block, a hole was created through the full thickness of the block (tunnel preparation) by using a low-speed pilot drill and the Er:YAG laser, in order to simulate the preparation for fixation screw site.

The holes were created through the full thickness of the block (tunnel preparation) for the both sample groups, which means ~ 4.5 mm, including cortical and spongy parts of the bone blocks. The first hole was prepared using a low-speed handpiece (1500 rpm) with a 1.0 mm wide pilot type stainless steel drill (Screw System, Meisinger, Neuss, Germany) under constant saline irrigation (Dental implant unit handpiece motor Surgic Xt plus Nsk, Japan). At the distance of 7 mm from the first hole, another tunnel preparation was performed using the variable square pulsed (VSP) Er:YAG laser and the RO2-C handpiece (AT Fidelis, Fotona, Ljubljana, Slovenia) under constant water spray cooling (30 mL/min). The Er:YAG laser operated in a noncontact mode at a distance of 7 mm from the bone surface. The laser parameters were: $\lambda = 2.94 \mu\text{m}$, power: 20 W, pulse energy: 1000 mJ, pulse repetition rate: 20 Hz, pulse duration: 300 ns, spot size: 0.9 mm.

During the preparations, both the laser articulated arm delivery system and the low-speed handpiece set were fixed. The bone plates were fixed with a clamp. To assure the blinded character of the study, bone sections and hole prep-

arations were performed by an expert in oral surgery (D.G.P.). Another operator (I.B.J.) marked the specimens before the preparations and performed all the measurements. Biosecurity standards to protect the personnel were followed.

FE-SEM

The morphological changes of the cortical and spongy surfaces of the tunnel preparations were analyzed under FE-SEM (FE-SEM, JSM-7000F, Jeol Ltd, Akishima, Tokyo, Japan) at resolutions of $25\text{--}15,000\times$ magnification, and an accelerating voltage of 20 kV. Following the preparation, the specimens were trimmed and cut under saline irrigation along the sagittal axis through the center of the each tunnel preparation using an electric round microcutting machine (Shandon Finesse, Shandon, England). Half of the samples from the laser and drill groups were randomly selected for FE-SEM. The samples were dehydrated in Shandon Excelsior ESTM tissue processor (Thermo Scientific, Cheshire, UK) using traditional reagents: serial concentrations of ethanol, xylol, and paraffin (Merck KgaA, Darmstadt, Germany). After the dehydration, the treated surfaces of the tunnel preparation were imaged uncoated using a cold cathode FE-SEM. The samples were previously pumped down in a vacuum desiccator until sufficient vacuum was achieved to obtain a micrograph.

SEM-EDX

The second half of each bone block was cast in plastic mold, with the treated surface facing the bottom of the mold. The molds were filled with Epo-Thin resin (Buehler, Lake Bluff, IL). Subsequently, the cast specimen was cured in a vacuum desiccator for 24 h. The internal surface of each tunnel preparation was polished with glass knives mounted on the microcutter (Reichert Ultracut S, Leica, Austria), until a flat, glass-like surface suitable for microanalysis was obtained. Qualitative EDX analysis of the irradiated and drilled bone surfaces was performed with an Oxford INCA Energy dispersive x-ray detector installed on the JEOL JSM-7000F, and using the Cameo software program (Cameo Chemicals, Cameo Software Suite, NOAA and EPA, USA). The elemental distribution of phosphorus (P), calcium (Ca), oxygen (O), carbon (C), magnesium (Mg), and sodium (Na) were determined. Composition scans were collected at randomly selected points in the cortical and spongy bone surfaces of the laser and drill tunnel preparations.

Semiquantitative EDX point analysis was performed in bone tissue surrounding the Er:YAG preparation (including cortical and spongy bone), and in the drill group, mapping was performed separately for the cortical and spongy parts. The levels (%) of P, Ca, O, C, Mg, and Na were determined. For each sample, a point on the cortical and spongy bone, as well as on the untreated bone tissue surrounding the preparations, was randomly selected, and the mean values for each position were calculated per group.

XRD

Cortical and spongy surfaces of the tunnel preparations and the untreated bone tissue surrounding the preparations (control) were analyzed using a powder x-ray monocrystal diffractometer (Oxford Diffraction Xcalibur Nova, Oxford

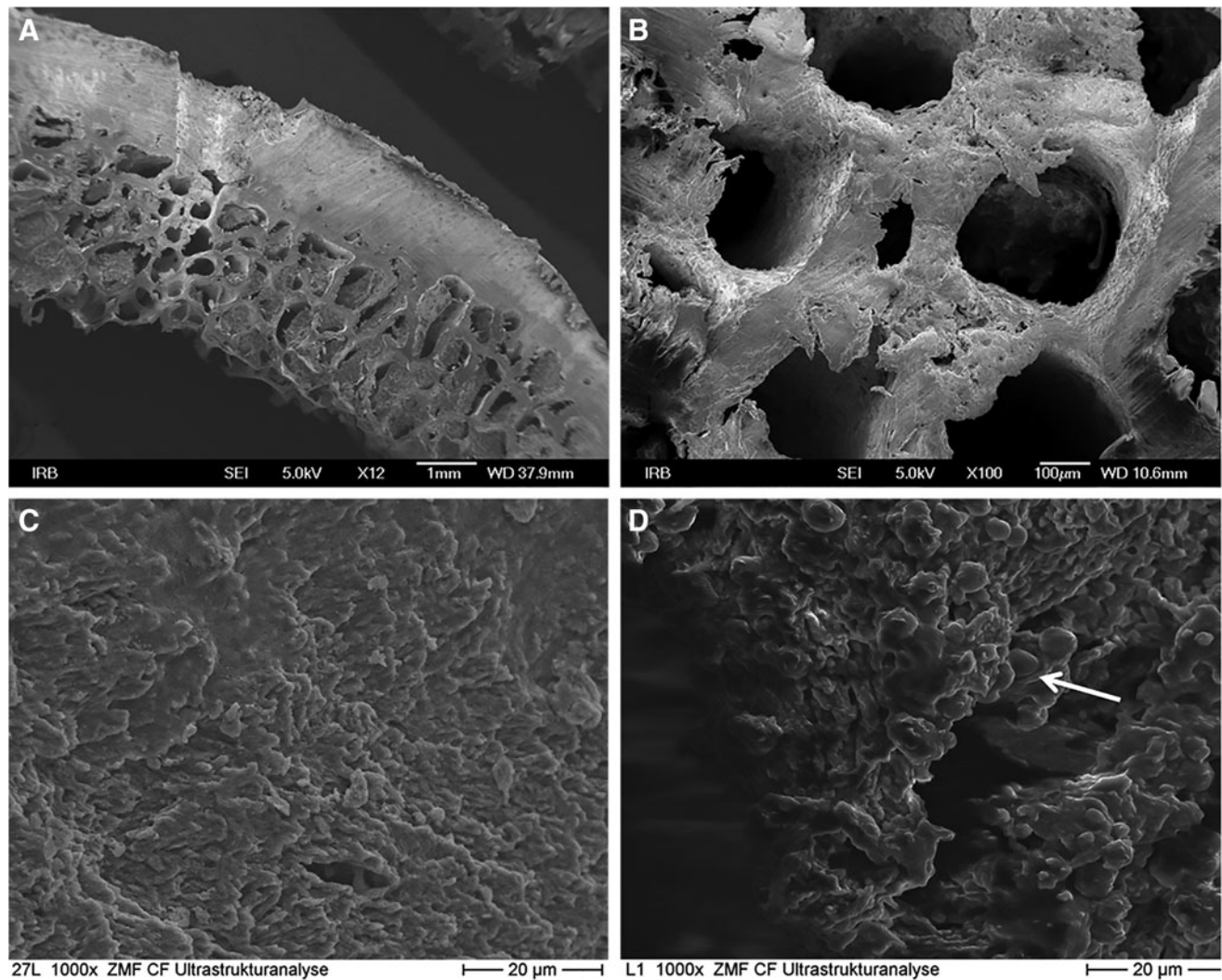


FIG. 1. Field emission scanning electron microscopy (FE-SEM) photomicrographs of Er:YAG laser ablation. (A) Well-defined sharp edges and knife-like cut with regular and empty intertrabecular spaces (12 \times magnification). (B) Empty intertrabecular spaces with unchanged trabecular bone (100 \times magnification). (C) Cortical surface with micro-irregularities and a rough, husky, and craggy appearance (1000 \times magnification). (D) spheric formations (arrow) on the trabecular bone, with a small amount of irregular and amorphous tissue (1000 \times magnification).

Diffraction Ltd, Poland, 2007) (DFX1) and a polycrystalline diffractometer (APD 2000, Ital Structures, Italy, 2007) (DFX2). With width of the beam of x-rays was 0.3 mm. Also, pure laboratory hydroxyapatite was used as a double control. After dehydration of the room temperature, during 48 h, cortical, spongy, and untreated parts of the tunnel preparations were pulverized into powder and stuffed into a glass capillary using a vacuum technique. A glass capillary with a diameter of 0.3 mm was constructed for the purposes of this study. Four frames per sample were recorded, with an exposure of 150 sec. The program CrysAlis PRO (Oxford Diffraction Ltd, Abingdon, UK, 2007) was used for data analysis.

Results

FE-SEM observations

Er:YAG laser. At low magnification, the Er:YAG laser preparations (L) were smooth, with well-defined sharp edges

and regular borders to the surrounding bone tissue (Fig. 1a). The spongy bone had empty intertrabecular spaces, without organic matrix, and with unchanged trabecular bone (Fig. 1b). At a higher resolution and magnification, the cortical bone was without the smear layer, rough, husky, and craggy, with micro-irregularities and without signs of carbonization or melting (Fig. 1c). On the spongy bone, fungiform shaped spheric formations with small amounts of irregular and amorphous parts of the tissue were found, without thermally induced changes (Fig. 1d).

Bur drilling. The drill preparations were full of bone fragments and fiber-like debris, and had irregular and not well-defined borders to the surrounding tissue (Fig. 2a). The spongy bone remained almost unchanged, with hairy irregularities on the surface of the trabecular bone and preserved organic matrix (Fig. 2a). At a higher magnification, the cortical bone was smooth, completely covered with

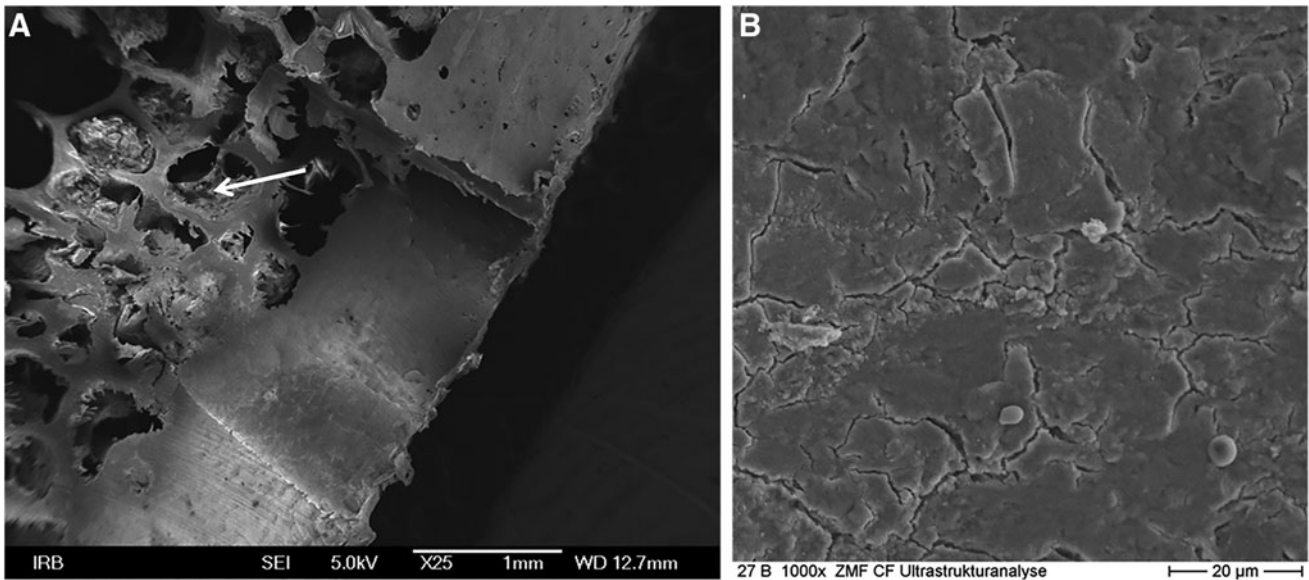


FIG. 2. Field emission scanning electron microscopy (FE-SEM) photomicrographs of bur drilling. (A) Irregular edges full of bone fragments and fiber-like debris, spongy bone with hairy-like irregularities on the surface of the trabecular bone and preserved organic matrix (arrow) ($25\times$ magnification). (B) Surface of the cortical bone completely covered with a smear layer and microcracks ($1000\times$ magnification).

smear layer and visible microcracks. At a higher magnification, a smear layer of variable thickness was placed all over the trabecular bone and intertrabecular spaces, without thermally induced changes. Microcracks and microfractures were rare, when compared with the cortical bone (Fig. 2b).

SEM/EDX observations

Figure 3 showed qualitative EDX analysis of the Er:YAG and the drill surface of the tunnel preparations. In bone tissue around the Er:YAG-irradiated preparation, the quantitative analysis (Fig. 4a) revealed the highest portion of C (40.68%) and O (34.37%) and a smaller amount of Ca (14.66%). Other elements were rare (P 8.87%, Na 1.12%, and Mg 0.30%). There were differences in the amount of the

chemical elements between cortical and spongy drilled bone tissue (Fig. 4b, c). In the cortical part, there was the highest portion of O (50.78%) and C (34.69%) and a smaller amount of P (14.53%), without Ca. In the spongy part, the analysis showed the highest amount of Ca (67.59%), and a smaller amount of C (12.02%), O (12.17%), P (7.67%) and Na (0.55%).

XRD observations

The XRD analysis did not reveal any differences in chemical composition between the Er:YAG-irradiated, the drilled, and the untreated bone (control) shown on diffractograms, and diffraction images (Fig. 5), when pure laboratory hydroxyapatite was used as a control. Also, there

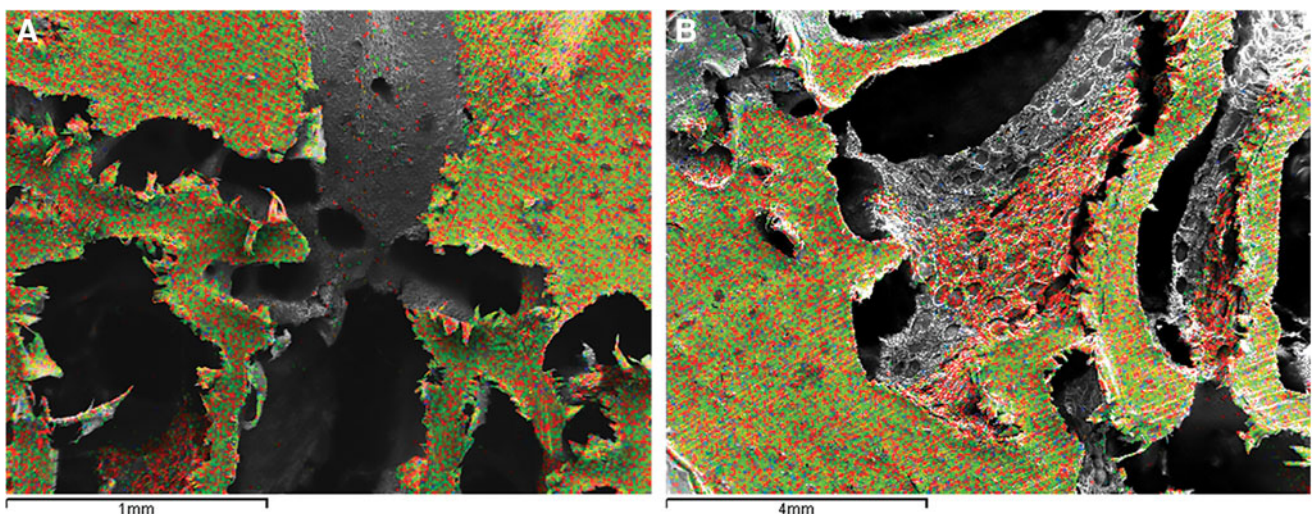
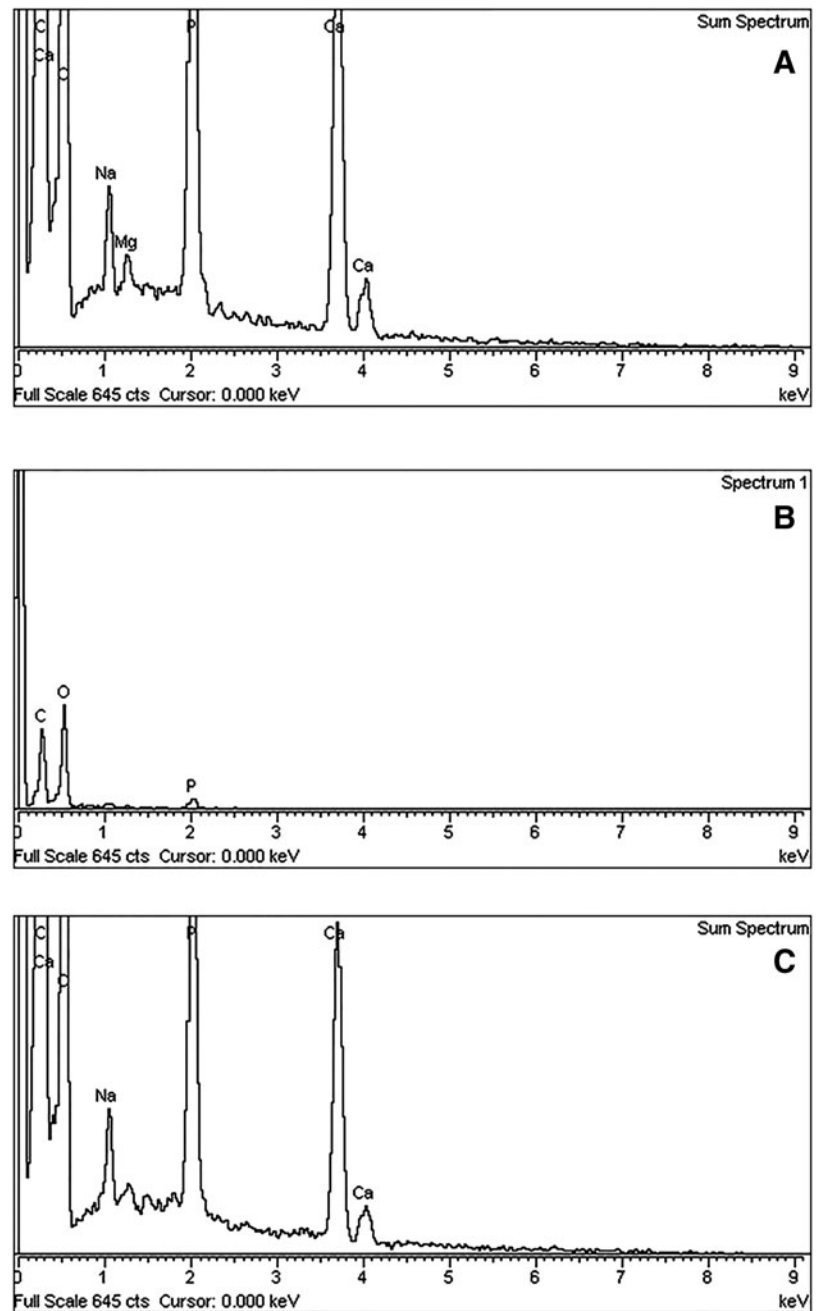


FIG. 3. Mapping of the chemical elements on the Er:YAG laser-irradiated site (A), and bur drilling site (B).

FIG. 4. Field emission scanning electron microscopy (FE-SEM)/ energy dispersive x-ray (EDX) analysis. **(A)** Er:YAG laser irradiation (1000 mJ/pulse, 20 Hz) under saline solution irrigation. **(B)** Cortical bone of bur drilling site. **(C)** Spongy bone of bur drilling site.



were no signs of thermally induced modifications of the hydroxyapatite crystals.

Discussion

The present *ex vivo* study evaluated the morphological and ultrastructural characteristics of the bone tissue after the Er:YAG laser and the conventional pilot drill osteotomy. FE-SEM observations showed that the Er:YAG ablation (power 20 W, pulse energy 1000 mJ, pulse repetition rate 20 Hz, pulse duration 300 μ s) is precise, with well-defined sharp edges and regular borders to the surrounding tissue, and without any sign of thermal damage. Similar findings were reported by Sasaki et al.,¹⁷ who also did not find areas of melting or carbonization in bone tissue after irradiation

with the Er:YAG laser (30–350 mJ/pulse, pulse repetition rate 20 Hz, pulse duration 200 μ s). In this study, the spherical formations on the cortical and the trabecular bone of the laser-ablated surface are, probably, a result of rapid growth of the temperature during laser irradiation, and then rapid cooling by the integrated cooling system of the laser device. Furthermore, the absence of a smear layer and the presence of micro-irregularities on the surface are a result of thermo-mechanical ablation, which depends significantly upon the amount of energy delivered during radiation. Because of the high absorption coefficient of the Er:YAG wavelength (2940 nm) in water and hydroxyl ions of hydroxyapatite,^{18–20} the bone or dental tissues absorb almost all energy delivered, which causes an immediate rise in local temperature. The heat vaporizes water, and internal positive pressure causes

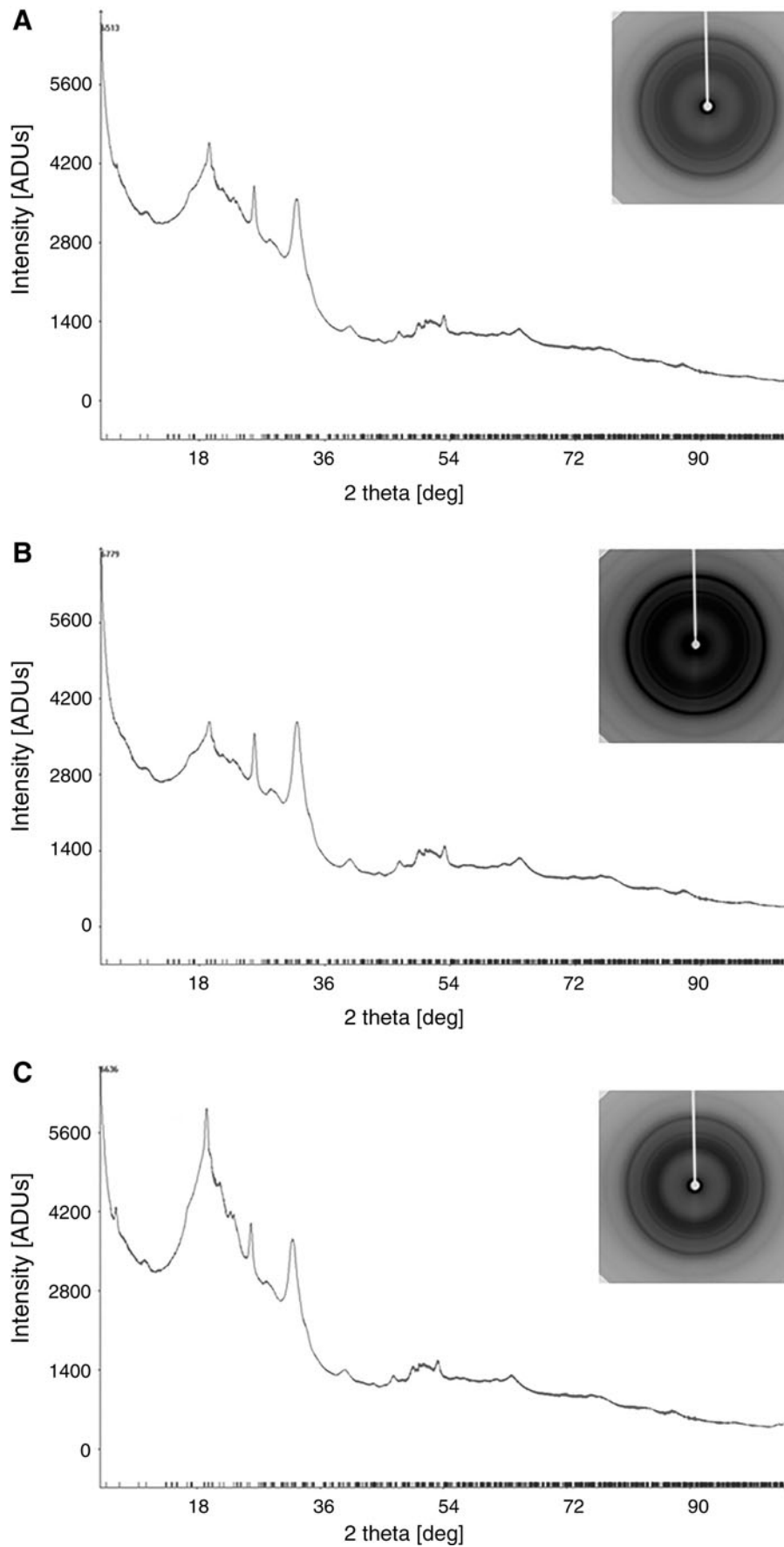


FIG. 5. Diffractograms and diffraction images of x-ray diffraction (XRD) analysis. **(A)** Er:YAG laser irradiation (1000 mJ/pulse, 20 Hz) under saline solution irrigation. **(B)** Cortical bone site after bur drilling. **(C)** Untreated bone tissue and pure hydroxyapatite.

micro-explosions and tissue ablation. Control of the extent of lateral damage during laser irradiation is based primarily on the speed of the laser application; the faster the pulse, the less the time available for conduction into adjacent tissue.²¹ Flash lamp pumped or optically pumped lasers, such as Er:YAG laser, can pulse faster than the tissue can begin to conduct heat laterally (i.e., the thermal relaxation time), thus minimizing lateral thermal damage.²¹

The response of biological tissue to laser irradiation depends significantly upon the nature of its components. Bone is basically composed of apatites surrounded by an organic matrix. The SEM/EDX analysis, in this study, showed similar amount and distribution of the chemical elements in the laser-irradiated site and in the untreated bone, which suggests that the Er:YAG ablation, under the settings used, did not cause any significant thermal damage. However, thermally induced morphological changes, fungiform-shaped spheric formations, are seen on the spongy part. A slightly reduced amount of calcium (14.66) probably occurred because the analysis included the cortical and spongy parts. Sasaki et al.²² demonstrated a changed layer that consisted of superficial intact tissue with numerous microcracks and slight recrystallization, and a deep, less affected layer. In another study by Sasaki et al.,¹⁷ chemical composition of laser-ablated bone tissue was analyzed with Fourier transform infrared (FTIR) spectroscopy, and the results also did not show any significant modifications in the composition compared with the untreated specimens. Only a loss of organic and a minor loss of inorganic components in the affected layer were found.^{20,23} In this study, FE-SEM analysis revealed empty intertrabecular spaces, which were a result of vaporization of the organic material. Sasaki et al.²² observed slightly increased levels of Ca and P at the superficial layer immediately below the irradiated surface, which was explained by the formation of some new products.²⁴ Other studies have demonstrated an increased, although not significant, Ca/P weight ratio in the Er:YAG and Er,Cr:YSGG laser-irradiated surface.^{23,25} In this study, there was no difference in the amount of Ca and P in bone tissue immediately below the laser-irradiated surface and bur-drilled bone. The difference among the results of the studies could be because of the different methodologies used, measurement sites, types of the lasers, and irradiation conditions, such as the use of coolant, irradiation power, and pulse repetition rate.^{22,26,27} The results in the drill group suggest the more significant impact of drilling on the cortical bone than on the spongy bone. The chemical distribution showed the presence of only organic material on the surface of cortical bone what is an evidence of the presence of smear layer demonstrated by FE-SEM.

According to our knowledge, this is the first study in which the x-ray diffraction method was used to evaluate the crystallographic changes of the bone tissue after laser ablation and drill osteotomies. The diffraction patterns of both the Er:YAG-lased and the bur-drilled specimens were basically similar to biological apatite and untreated bone, which tallies with the results of SEM/EDX analysis, and rejects any carbonization effect. Sasaki et al.²² analyzed bone tissue with the electron diffraction method, and also did not find differences in apatite structure after the Er:YAG and the drill osteotomies. A similar chemical composition of

bone tissue after the bur drilling and laser ablation, in this study, clearly indicates the high suitability of the Er:YAG laser for the removal of hard tissues. Moreover, the well-defined edges of the preparation and the unique surface without the smear layer produced by Er:YAG laser ablation may potentially enhance the adhesion of blood elements at the start of the healing process.⁸ Namely, it has already been reported that the smear layer may act as a barrier preventing blood element interaction with the underlying tissue, resulting in a prolonged healing process.²⁸

Conclusions

The results of this study showed that Er:YAG laser ablation, with the parameters used in this study, did not cause any chemical or crystallographic changes of the bone tissue. Compared with the drill, Er:YAG laser created well-defined preparation edges and no smear layer in cortical bone.

Acknowledgments

We gratefully acknowledge Fotona for laser usage, and Janez Žabkar for help during laser preparation. This study was performed and financed within the research project "Experimental and Clinical Endodontology," no. 065-0650444-0418, approved by the Ministry of Science, Education, and Sport of the Republic of Croatia. The authors acknowledge Fotona d.d., Slovenia and Institute for Physics, Zagreb, Croatia for support and assistance.

Author Disclosure Statement

No competing financial interests exist.

References

1. Stopp, S., Deppe, H., and Lueth, T. (2008). A new concept for navigated laser surgery. *Lasers Med. Sci.* 23, 261–266.
2. Rupperecht, S., Tangermann, K., Kessler, P., and Neukam, F.W., and Wiltfang, J. (2003). Er:YAG laser osteotomy directed by sensor controlled systems. *J. Craniomaxillofac. Surg.* 31, 337–342.
3. Papadaki, M., Doukas, A., Farinelli, W.A., Kaban, L., and Troulis, M. (2007). Vertical ramus osteotomy with Er:YAG laser: a feasibility study. *Int. J. Oral Maxillofac. Surg.* 36, 1193–1197.
4. Hohlweg-Majert, B., Deppe, H., Metzger, M.C., Stopp, S., Wolff, K.D., and Lueth, T.C. (2010). Bone treatment laser-navigated surgery. *Lasers Med. Sci.* 25, 67–71.
5. Stübinger, S., Landes, C., Seitz, O., and Sader, R. (2007). Er:YAG laser osteotomy for intraoral bone grafting procedures: a case series with a fiber-optic delivery system. *J. Periodontol.* 78, 2389–2394.
6. Li, Z.Z., Reinisch, L., and Van de Merwe, W.P. (1992). Bone ablation with Er:YAG and CO₂ laser: study of thermal and acoustic effects. *Lasers Surg. Med.* 12, 79–85.
7. Kayano, T., Ochiai, S., Kiyono, K., Yamamoto, H., Nakajima, S., and Mochizuki, T. (1991). Effect of Er:YAG laser irradiation on human extracted teeth. *J. Clin. Laser Med. Surg.* 9, 147–150.
8. Stübinger, S. (2010). Advances in bone surgery: the Er:YAG laser in oral surgery and implant dentistry. *Clin. Cosmet. Investig. Dent.* 2, 47–62.
9. Gabrić Pandurić, D., Bago, I., Katanec, D., Žabkar, J., Miletić, I., and Anić, I. (2012). Comparison of Er:YAG laser

- and surgical drill for osteotomy in oral surgery: an experimental study. *J. Oral Maxillofac. Surg.* 70, 2515–2521.
10. Stübinger, S., Nuss, K., Landes, C., von Rechenberg, B., and Sader, R. (2008). Harvesting of intraoral autogenous block grafts from the chin and ramus region: preliminary results with a variable square pulse Er:YAG laser. *Lasers Surg. Med.* 40, 312–318.
 11. Stübinger, S., von Rechenberg, B., Zeilhofer, H.F., Sader, R., and Landes, C. (2007). Er:YAG laser osteotomy for removal of impacted teeth: clinical comparison of two techniques. *Lasers Surg. Med.* 39, 583–588.
 12. Romeo, U., Del Vecchio, A., Palaia, G., Tenore, G., Visca, P., and Maggiore, C. (2009). Bone damage induced by different cutting instruments – an in vitro study. *Braz. Dent. J.* 20, 162–168.
 13. de Mello, E.D., Pagnoncelli, R.M., Munin, E., Filho, M.S., de Mello, G.P., Arisawa, E.A., and de Oliveira, M.G. (2008). Comparative histological analysis of bone healing of standardized bone defects performed with the Er:YAG laser and steel burs. *Lasers Med. Sci.* 23, 253–260.
 14. Lewandrowski, K.U., Lorente, C., Schomacker, K.T., Flotte, T.J., Wilkes, J.W., and Deutsch, T.F. (1996). Use of the Er:YAG laser for improved plating in maxillofacial surgery: comparison of bone healing in laser and drill osteotomies. *Lasers Surg. Med.* 19, 40–45.
 15. Peavy, G.M., Reinisch, L., Payne, L.T., and Venugopalan, V. (1999). Comparison of cortical bone ablations by using infrared laser wavelengths 2.9 to 9.2 microm. *Lasers Surg. Med.* 25, 421–434.
 16. Spencer, P., Payne, J.M., Cobb, C.M., Reinisch, L., Peavy, G.M., Drummer, D.D., Suchman, D.L., and Swafford, J.R. (1999). Effective laser ablation of bone based on the absorption characteristics of water and proteins. *J. Periodontol.* 70, 68–74.
 17. Sasaki, K.M., Aoki, A., Ichinose, S., Yoshino, T., Yamada, S., and Ishikawa, I. (2002). Scanning electron microscopy and Fourier transformed infrared spectroscopy analysis of bone removal using Er:YAG and CO₂ lasers. *J. Periodontol.* 73, 643–652.
 18. Keller, U., and Hibst, R. (1989). Experimental studies of the application of the Er:YAG laser on dental hard substances: II. Light microscopic and SEM investigations. *Lasers Surg. Med.* 9, 345–351.
 19. Hibst, R., and Keller, U. (1989). Experimental studies of the application of the Er:YAG laser on dental hard substances: I. Measurement of the ablation rate. *Lasers Surg. Med.* 9, 338–344.
 20. Hibst, R. (1992). Mechanical effects of Er:YAG laser bone ablation. *Lasers Surg. Med.* 12, 125–130.
 21. Trost, D., Zacherl, A., and Smith, M. (1992). Surgical laser properties and their tissue interaction. St. Louis: Mosby-Year Book.
 22. Sasaki, K.M., Aoki, A., Ichinose, S., and Ishikawa, I. (2002). Ultrastructural analysis of bone tissue irradiated by Er:YAG Laser. *Lasers Surg. Med.* 31, 322–332.
 23. Kuroda, S., and Fowler, B.O. (1984). Compositional, structural, and phase changes in *in vitro* laser-irradiated human tooth enamel. *Calcif. Tissue Int.* 36, 361–369.
 24. Tokonabe, H., Kouji, R., Watanabe, H., Nakamura, Y., and Matsumoto, K. (1999). Morphological changes of human teeth with Er:YAG irradiation. *J. Clin. Laser. Med. Surg.* 17, 7–12.
 25. Kimura, Y., Yu, D.G., Fujita, A., Yamashita, A., Murakami, Y., and Matsumoto, K. (2001). Effects of erbium:chromium:YSGG laser irradiation on canine mandibular bone. *J. Periodontol.* 72, 1178–1182.
 26. Nelson, J.S., Orenstein, A., Liaw, L.H., and Berns, M.W. (1989). Mid-infrared erbium:YAG laser ablation of bone: The effect of laser osteotomy on bone healing. *Lasers Surg. Med.* 9, 362–374.
 27. El Montaser, M.A., Devlin, H., Sloan, P., and Dickinson, M.R. (1997). Pattern of healing of calvarial bone in the rat following application of the erbium:YAG laser. *Lasers Surg. Med.* 21, 255–261.
 28. Visuri, S.R., Walsh, J.T. Jr., and Wigdor, H.A. (1996). Erbium laser ablation of dental hard tissue: Effect of water cooling. *Lasers Surg. Med.* 18, 294–300.

Address correspondence to:
 Dragana Gabrić Pandurić
 Department of Oral Surgery
 School of Dental Medicine
 University of Zagreb
 Gundulićeva 5
 10000 Zagreb
 Croatia

E-mail: dgabric@sfzg.hr